Inorganic Chemistry

ARTICLE

pubs.acs.org/IC

# Complexation of Lanthanides(III), Americium(III), and Uranium(VI) with Bitopic N,O Ligands: an Experimental and Theoretical Study

Cécile Marie,[†] Manuel Miguirditchian,[*,†] Dominique Guillaumont,[†] Arnaud Tosseng,[†] Claude Berthon,[†] Philippe Guilbaud,[†] Magali Duvail,[†] Julia Bisson,[†] Denis Guillaneux,[†] Muriel Pipelier,[‡] and Didier Dubreuil[‡]

[†]CEA, Nuclear Energy Division, RadioChemistry & Processes Department, SCPS, F-30207 Bagnols-sur-Cèze, France

[‡]Chimie Et Interdisciplinarité, Synthèse, Analyse, Modélisation (CEISAM), UFR des Sciences et des Techniques, Université de Nantes, UMR CNRS 6230, 2 rue de la Houssinière, F-44322 Nantes, France

Supporting Information

**ABSTRACT:** New functionalized terpyridine-diamide ligands were recently developed for the group actinide separation by solvent extraction. In order to acquire a better understanding of their coordination mode in solution, protonation and complexation of lanthanides(III), americium(III), and uranium(VI) with these bitopic N,O-bearing ligands were studied in homogeneous methanol/water conditions by experimental and theoretical approaches. UV−visible spectrophotometry was used to determine the protonation and stability constants of te-tpyda and dedp-tpyda. The conformations of free and protonated forms of te-tpyda were investigated using NMR and theoretical calculations. The introduction of amide functional groups on the terpyridine moiety improved the extracting properties of these new ligands by lowering their basicity and enhancing the stability of the corresponding 1:1 complexes with lanthanides(III). Coordination of these ligands was studied by density functional theory and molecular dynamics calculations, especially to evaluate potential participation of hard oxygen and soft nitrogen atoms in actinide coordination and to correlate with their affinity and selectivity. Two predominant inner-sphere coordination modes were found from the calculations: one mode where the cation is coordinated by the nitrogen atoms of the cavity and by the amide oxygen atoms and the other mode where the cation is only coordinated by the two amide oxygen atoms and by solvent molecules. Further simulations and analysis of UV−visible spectra using both coordination modes indicate that inner-sphere coordination with direct complexation of the three nitrogen and two oxygen atoms to the cation leads to the most likely species in a methanol/water solution.

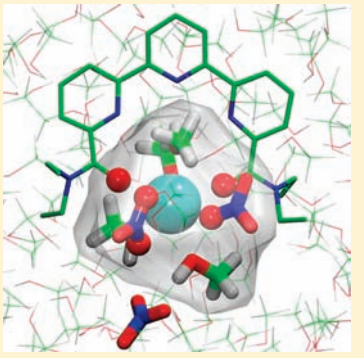

## INTRODUCTION

The separation of actinides (U, Np, Pu, Am, and Cm) from fission products (especially actinides(III) from lanthanides(III)) is a key step for the reduction of radiotoxicity and thermal emissions of ultimate nuclear waste. The separation of light actinides (U, Np, and Pu) from lanthanides (Ln) can be achieved by exploiting the greater affinity of the higher oxidation states of the light 5f elements with hard Lewis bases (according to the Pearson HSAB classification),[1] which form complexes with a metal−ligand bond, largely electrostatic in nature. However, transplutonium actinide ($Am^{III}$ and $Cm^{III}$) and lanthanide(III) cations have very close physicochemical properties. They are both strongly hydrated[2] and present similar ionic radii.[3,4] Their interactions with inorganic and organic ligands are predominantly determined by electrostatic and steric factors. Even if actinides(III) ($An^{III}$) are considered to be hard acids in HSAB theory, they are expected to form bonds having a slightly higher covalent character with softer Lewis bases. This electronic effect would be attributed to the ability of actinide valence orbitals, especially 5f, to participate in bonding, whereas the lanthanide 4f orbitals are lower in energy and less spatially expanded. Efficient extractants for the separation of $An^{III}$ from $Ln^{III}$ contain soft sulfur donors[5−8] and soft nitrogen donors. Tridentate nitrogen-donor aromatic bases, such as 2,6-bis(5,6-dialkyl-1,2,4-triazin-3-yl)pyridine (Rbtp), 2,4,6-tris(pyridin-2-yl)-1,3,5-triazine (tptz), 2-amino-4,6-bis(pyridin-2-yl)-1,3,5-triazine (adptz), and 2,2′:6′2″-terpyridine (tpy) are some of the most extensively investigated nitrogen-donor ligands.[9] They are expected to form bonds with a slightly greater covalent character with $An^{III}$ than with $Ln^{III}$.[10]

We have recently reported the synthesis of bitopic N,O ligands *N*,*N*,*N*′,*N*′-tetrabutyl-6,6″-(2,2′:6′,2″-terpyridine)diamide (tb-tpyda) and *N*,*N*,*N*′,*N*′-tetraoctyl-6,6″-(2,2′:6′,2″-terpyridine)diamide (to-tpyda), which can separate $U^{VI}$, $Np^{V,VI}$, $Pu^{IV}$, $Am^{III}$, and $Cm^{III}$ by solvent extraction with selectivity for actinides over lanthanides ($2 < SF_{An^{III}/Ln^{III}} < 15$) from 3 M $HNO_3$ solutions in the absence of a synergist.[11] These ligands consist of two units of different nature: the tpy moiety with soft nitrogen donors, which should induce $An^{III}/Ln^{III}$ selectivity, and two amide groups with hard oxygen donors, which should enhance complex stability and ligand solubility in diluents. Understanding the separation and extraction behavior of these terpyridine-diamide

**Received:** February 8, 2011
**Published:** June 10, 2011

  

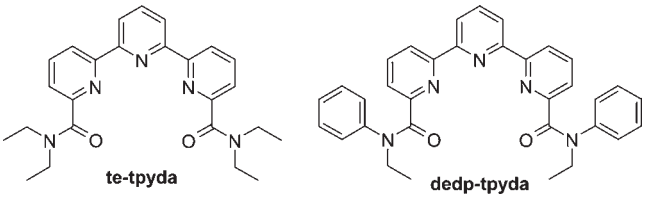


**Figure 1.** Structure of the new functionalized tpy ligands.

ligands can be aided by a better knowledge of their complexation mode in homogeneous media. In this investigation, the complexation properties of *N,N,N′,N′*-tetraethyl-6,6′′-(2,2′:6′,2′′-terpyridine)diamide (te-tpyda) and *N,N′*-diethyl-*N,N′*-diphenyl-6,6′′-(2,2′:6′,2′′-terpyridine)diamide (dedp-tpyda) (Figure 1) have been studied in homogeneous methanol or methanol/water conditions.

The aim of this study is to determine the influence of tpy functionalization by amide groups on the ligand basicity, ligand conformation, actinide affinity, and $An^{III}/Ln^{III}$ selectivity. The protonation and complexation constants of te-tpyda and dedp-tpyda with $Ln^{III}$, $Am^{III}$, and $U^{VI}$ were determined by UV−visible spectrophotometry and compared to tpy constants. The possible conformations of free tpy and te-tpyda molecules in solution were studied by quantum chemistry calculations using density functional theory (DFT) and by nuclear magnetic resonance (NMR). DFT calculations and molecular dynamics (MD) simulations were adopted to gain a better understanding of the coordination mode of these ligands, especially to evaluate the potential participation of hard oxygen and soft nitrogen atoms in actinide coordination and to correlate with their affinity and selectivity.

## EXPERIMENTAL SECTION

**Materials.** The ligands te-pyda and dedp-tpyda were prepared according to the synthesis described in a previous study.[11] Stock solutions ($7.5 \times 10^{-2}$ mol·L$^{-1}$) of te-pyda and dedp-tpyda were prepared by dissolution of the compounds in high-performance liquid chromatography (HPLC)-grade methanol (MeOH). Lanthanide (La, Nd, Eu, and Yb) chloride stock solutions were prepared by dissolution of 99.9% $LnCl_3 \cdot 6H_2O$ (Aldrich) in pure water ($H_2O$). The $Ln^{3+}$ concentration in each stock solution was measured using a Jobin-Yvon inductively coupled plasma atomic emission spectrometry (ICP-AES) spectrometer against standard solutions of the lanthanide cations. The uranium stock solution was prepared by dissolution of depleted uranium(VI) nitrate (Prolabo) in $H_2O$. Uranium hydroxide was then precipitated using sodium hydroxide, washed, and redissolved in dilute hydrochloric acid (HCl). The $UO_2^{2+}$ concentration in this stock solution was measured by X-ray fluororescence. The americium stock solution was prepared by the dissolution of $AmO_2$ (99.99 mol % Am-241) in $HNO_3$ followed by $Am^{III}$ purification using a Dowex-50 cation-exchange resin. $Am^{3+}$ in 0.1 M $HNO_3$ was sorbed onto the resin, washed several times with 0.1 M $HNO_3$, and eluted with 5 M $HNO_3$. Americium hydroxide was then precipitated by adding sodium hydroxide, washed, and redissolved in dilute HCl. The $Am^{3+}$ concentration in this stock solution (0.019 M) was measured by α and γ spectrometry.

**Preparation of Solutions.** The samples were prepared by the addition of weighed amounts of the ligand (te-pyda, dedp-tpyda, or tpy) and hydrochloric acid (HCl), lanthanide, or actinide stock solutions and of sufficient $H_2O$ and MeOH to maintain a constant 71/29 mass % MeOH/$H_2O$ ratio and to take into account the volume contraction between $H_2O$ and MeOH. The density of the stock solutions and the samples were measured with an Anton Paar densimeter to transpose to the volume proportions (corresponding to 75/25 vol %). The density of the americium solution was assumed to be equal to that of the lanthanide solution at similar metal concentration. The pH of the metal/ligand samples in MeOH/$H_2O$ was systematically measured between 3.5 and 5 even for the more concentrated cation solution. According to the low p$K_a$ values measured with these ligands, the pH of the titration is thus high enough to neglect the metal/proton competition and stability constants were not corrected by the p$K_a$. Background electrolytes were not added to the solutions to control the ionic strength because trial runs indicated that interactions between polyaromatic ligands and common alkali-metal cations would skew the measured thermodynamic parameters. However, given the low concentrations of the neutral ligand and metal ions ($10^{-5}$−$10^{-2}$ mol·L$^{-1}$), the ratio of the solute activity coefficients was considered constant. This hypothesis is not valid in the case of the determination of protonation constants because concentrated HCl was used and thus changed the ionic strength from almost 0 to 2.6 M. The protonation constants calculated here are therefore conditional and cannot be directly linked to the metal constants.

**Table 1. Conditional Protonation Constants of te-tpyda, dedp-tpyda, and tpy Measured at 21 °C in 75/25 vol % MeOH/$H_2O$, Chloride Media, and Variable Ionic Strength ($I$ = 0−2.6 M)[a]**

| | ligand | | | |
|---|---|---|---|---|
| | te-tpyda | dedp-tpyda | tpy | tpy[a,27] |
| log $K_{1H}$ | 1.0 ± 0.1 | 1.0 ± 0.2 | 3.3 ± 0.1 | 3.5 |
| log $K_{2H}$ | not observed | not observed | 1.7 ± 0.1 | 1.7 |

[a] Measured at 25 °C.

**Spectrophotometric Studies.** Spectrophotometric titrations of the proton, lanthanides, and uranium were carried out with a Cary 5 spectrophotometer, while americium experiments were performed using a Shimadzu 3101 spectrophotometer in a glovebox. Protonation and lanthanide complexation were studied by following the ligand $\pi-\pi^*$ absorption bands (200−400 nm) with increasing acidity or concentrations of the metal ion, respectively, while neodymium, uranium, and americium complexation were studied by following the metal f−f absorption band (450−900 nm for Nd, 400−500 nm for U, and 503 nm for Am). Typically, between 9 and 10 samples (with different metal/ligand ratios) were used for the lanthanide titrations, while 8 and 7 samples were used for americium and uranyl titration, respectively. Protonation and complex stability constants were calculated by fitting the experimental absorbencies and molar absorptivities of the absorbing species by factorial analysis using the *Hyperquad 2006* program.[12] Depending on the system, between 200 and 300 nm wavelengths were used in the calculations. Each constant was calculated based on one titration. The fitting program calculates an uncertainty based on the difference between the experimental and calculated absorbencies. These values were systematically very low (≤0.02), confirming the hypothesis on the speciation of species. However, they underestimated the real uncertainties due to experimental errors. The uncertainties given in Tables 1 and 2 were calculated by taking into account a 10% error on the concentrations of the ligand and cation and performing again the experimental data fitting with *Hyperquad 2006*, taking into account the concentrations ±10% for each reactant. These values correspond to a 95% confidence level ($2\sigma$).

**NMR Experiments.** Two-dimensional $^{15}N$ NMR spectra (gHMBC pulse sequence) and nuclear Overhauser effect (NOE) experiments (NOESY one-dimensional pulse sequence) were performed on a 400 MHz Varian Inova spectrometer with a 5 mm Z-gradient HCX reverse probe. MeOH and $H_2O$ used were $CD_3OD$ (99.8+ atom % D)


dx.doi.org/10.1021/ic200271e |*Inorg. Chem.* 2011, 50, 6557–6566

**Table 2. Stability Constants ($\log \beta_1$) for 1:1 Lanthanide(III), Americium(III), and Uranyl Complexes with te-tpyda, dedp-tpyda, and tpy in 75/25 vol % MeOH/$H_2O$, Chloride Media at 21°C[a]**

| | cation | | | | | |
|---|---|---|---|---|---|---|
| | $La^{3+}$ | $Nd^{3+}$ | $Eu^{3+}$ | $Yb^{3+}$ | $Am^{3+}$ | $UO_2^{2+}$ |
| $\log \beta_1$(te-tpyda) | $2.7 \pm 0.1$ | $4.2 \pm 0.1$<br>$3.7 \pm 0.1$[a] | $4.5 \pm 0.1$ | $3.7 \pm 0.1$ | $3.8 \pm 0.1$[a] | $2.4 \pm 0.1$[a] |
| $\log \beta_1$(dedp-tpyda) | | | $5.0 \pm 0.1$ | | | |
| $\log \beta_1$(tpy) | 1.6[27] | $2.7 \pm 0.1$ | $2.5 \pm 0.1$ | | | |

[a] Determined by following the absorption of the cation in the visible domain.

and $D_2O$ (99.9+ atom % D) to readily observe protons of the ligand at a 0.01 mol·$L^{-1}$ concentration. $CH_3NO_2$ was added to the MeOH/$H_2O$ stock solution to get a reference signal for $^1H$ (set at 4.33 ppm) and $^{15}N$ (set at 0 ppm) NMR spectra. All NMR measurements were acquired at 25 °C.

**Computational Details.** Quantum chemistry calculations were carried out in the framework of DFT with the *Gaussian 03* package.[13] For each molecular species (free ligands and lanthanide or actinide complexes), a geometry optimization was first performed in the gas phase. A vibrational frequency analysis was then carried out analytically in order to confirm the minimum energy and determine the thermal corrections. From the thermal corrections and electronic energies, the Gibbs free energy of each species was calculated in the gas phase. Finally, solvation Gibbs free energies were obtained from single-point energy calculations for the gas-phase-optimized structure in the presence of a polarizable continuum model to describe solvent effects. Energy differences between structural isomers were analyzed using their Gibbs energy differences determined in the gas phase and in solution. The electronic transition energies and oscillator strengths were determined from time-dependent DFT (TD-DFT) calculations on the gas-phase-optimized geometry but in the presence of a continuum solvent model. Unless stated otherwise, in all calculations, the hybrid B3LYP functional was employed. For open-shell systems, an unrestricted DFT method was used. For neodymium and americium, relativistic effects were taken into account through relativistic effective core potentials (RECPs). For neodymium, unless stated otherwise, large-core energy-adjusted 4f-in-core pseudopotentials developed in the Stuttgart and Dresden groups were used, together with the accompanying segmented basis set, to describe the valence electron density.[14−16] Large-core RECPs put 5s, 5p, 6d, and 6s shells in the valence space. Small-core RECPs replace 60 core electrons for actinides and 28 electrons for the lanthanides. The corresponding valence basis sets associated with small-core pseudopotentials are (14s13p10d8f) contracted to [10s8p5d4f] for lanthanides and (12s11p9d8f) contracted to [8s7p6d4f] for actinides. The basis set associated with lanthanide large-core pseudopotentials is (7s6p5d) contracted to [5s4p3d]. Two diffuse f functions were added. For americium, the newly developed "large core" or 5f-in-core pseudopotential was used with (7s6p5d2f) contracted to [5s4p3d2f].[17] On other atoms, the 6-31G* basis set was employed for geometry optimizations. Single-point energy and TD-DFT calculations were done with the larger 6-311+G(d,p) basis set. In *Gaussian 03*, the grid parameter, which specifies the integration grid used for numerical integrations, was set to ultrafine. Solvent effects were estimated through a polarizable continuum model (IEFPCM in *Gaussian 03*) in which the molecular cavity was constructed using a series of overlapping spheres using UAHF radii.

MD simulations of Ln(te-tpyda)$(NO_3)_3$ ($Ln^{3+}$ = $Nd^{3+}$ and $Dy^{3+}$) were carried out with *AMBER 8*,[18] using explicit polarization. $Nd^{3+}$ and $Dy^{3+}$ have been selected in order to be able to compare the coordination sphere for two cations of different sizes in the lanthanide series. These cations indeed have structural characteristics representative of both the first and second halves of this series ($Nd^{3+}$ and $Dy^{3+}$ are surrounded respectively by nine and eight $H_2O$ molecules in their first coordination sphere in a dilute $H_2O$ solution). $H_2O$ and MeOH explicit solvents were simulated using periodic boundary conditions on the simulation box, and long-range interactions were calculated using the particle-mesh Ewald method.[19] Equations of motion were numerically integrated using a 1 fs time step. Systems were equilibrated over at least 100 ps before 2 ns production runs. The $Ln^{III}$ cations parameters were determined by reproducing the experimental structural properties of molecules and ions in solution,[20] using atomic polarizabilities calculated by Clavaguéra and Dognon.[21] $H_2O$ molecules were described by the polarizable rigid POL3 model.[22,23] $NO_3^-$ anions were described by the polarizable model defined in our previous study, providing structural properties of $NO_3^-$ in reasonable agreement with published structural data.[20] The Optimized Potentials for Liquid Simulations all-atom AMBER force field was used to model MeOH and terpyridinediamide molecules.[24] Atomic partial charges on MeOH molecules determined by Yu et al. in their polarizable COS/M model were used.[25] These sets of parameters allow reproductibility of the experimental density of neat MeOH ($d_{MD}$ = 0.803 vs $d_{exp}$ = 0.787). Atomic partial charges on the functionalized tpy molecule were calculated with the restricted electrostatic potential procedure[26] (Figure 2).

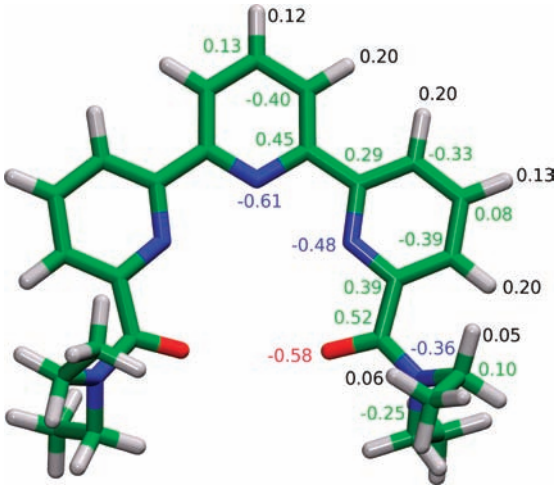


**Figure 2.** Atomic partial charges on te-tpyda used for MD simulations.

For all of the MD simulations, the lanthanide nitrate salts were built as first-shell dissociated salts. At the beginning of the simulations, the $Ln^{3+}$ cations were located in the tpy cavity.

## RESULTS

**Basicity and Conformation of Terpyridinediamides.** *Basicity of te-tpyda and dedp-tpyda Determined by UV−Visible Spectrophotometry.* The protonation constants of te-tpyda,


dx.doi.org/10.1021/ic200271e |*Inorg. Chem.* 2011, 50, 6557–6566

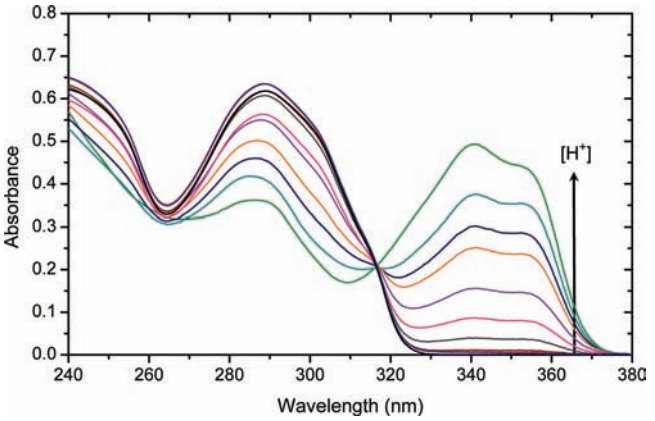


**Figure 3.** Spectrophotometric titration of a $2.7 \times 10^{-5}$ mol·L$^{-1}$ te-tpyda solution with increasing concentrations of HCl in 75/25 vol % MeOH/$H_2O$ at 21 °C. Path length: 1 cm. 0.42 < pH < 7.00.

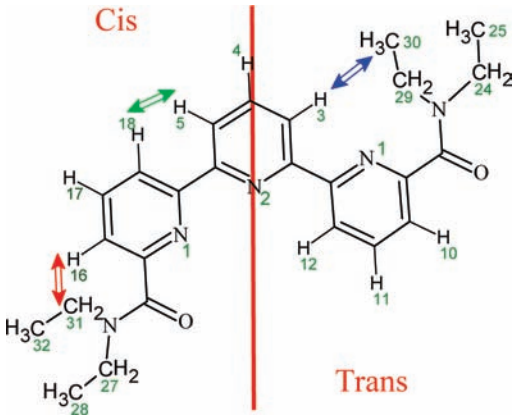


**Figure 4.** Cis and trans configurations of the lateral pyridines that explain the observed NOE of te-tpyda in 75/25 vol % MeOH/$H_2O$.

dedp-tpyda, and tpy were determined using UV−visible spectrophotometry by titrating the ligands with HCl in 75/25 vol % MeOH/$H_2O$ at 21 °C. The protonation constants $K_{iH}$ are defined by equilibrium (1).

$$H_{i-1}L^{(i-1)+} + H^+ \overset{K_{iH}}{\rightleftharpoons} H_iL^{i+} \quad (1)$$

Hydrochloric acid was used instead of nitric acid because chloride anions do not absorb in UV and are very weak ligands toward lanthanide cations. The addition of HCl (from 0 to 2.6 mol·L$^{-1}$) led to spectral modifications due to protonation of the molecule. The spectrophotometric titrations of te-tpyda and dedp-tpyda by HCl are shown in Figure 3 and in the Supporting Information, respectively. Conditional protonation constants $K_{1H}$ were calculated from the set of UV absorption spectra over a wavelength range of 200−400 nm using *Hyperquad 2006*. The results are reported in Table 1 and compared with tpy protonation constants determined previously in the same conditions and with the same technique.[27]

The tpy protonation constants measured in this work are slightly different from previously published results also determined by UV−visible spectrophotometry.[27] The slight difference in the value of the first protonation constant (0.2 logarithmic units) may be due to a different mathematic treatment of the spectrophotometric data. Only one protonated complex was observed in the case of te-tpyda and dedp-tpyda, while the spectrophotometric data were correctly fitted with two protonated species in the case of tpy. These results are consistent with the presence of an isosbestic point for te-tpyda (Figure 3) and dedp-tpyda titrations, while no such isosbestic point was observed with tpy.[27]

*NMR Study of te-tpyda and tpy Protonation.* $^{15}N-^{1}H$ correlation spectra (gHMBC pulse sequence) of tpy and te-tpyda were recorded in 75/25 vol % $CD_3OD/D_2O$ at 25 °C, with and without DCl, in order to identify the protonation sites. Spectra are provided in the Supporting Information. Three protonation sites are available on tpy and te-tpyda ligands: one N2 nitrogen atom on the central pyridine and two N1 nitrogen atoms on the lateral pyridines (the numbering of te-tpyda atoms is reported in Figure 4). According to $^{15}N$ NMR spectra, their behavior toward the acidic proton differs greatly from one ligand to another. Without DCl in the MeOH/$H_2O$ medium, $^{15}N$ chemical shifts are −83.4 ppm for N1 and N2 of te-tpyda and −82.7 and −86.8 ppm for N1 and N2 of tpy, respectively. In the presence of 0.32 mol·L$^{-1}$ DCl, N1 nitrogen atoms of tpy undergo a variation of 95.9 ppm, while the N2 atom undergoes a variation of only 9.9 ppm. This large change in the N1 chemical shift compared to those of N2 can be explained by the tpy protonation through nitrogen atoms on the lateral pyridines. In the case of te-tpyda, a large shift of 112.8 ppm is also observed with N2, while the N1 nitrogen atoms undergo a shift of only 15.2 ppm. This result clearly shows that the te-tpyda protonation site is different from the tpy one and occurs on the N2 nitrogen atom of the central pyridine.

To go further, NOE experiments (NOESY1D pulse sequence) have been carried out in order to get some conformational information on te-tpyda in MeOH/$H_2O$ media. Without DCl, the NOE between two adjacent pyridine ring protons (H18 and H5 in Figure 4) proves that a cis conformation (between the central pyridine ring and one lateral pyridine) exists in solution. Nevertheless, the trans conformation of the pyridine rings exists as well because NOE effects are observed between two protons of one ethyl group (H29 and H30) and one proton of the central pyridine (H3). Thanks to this phenomenon, the chemical shift assignments of $CH_2$ and $CH_3$ amide groups were straightforward. Indeed, protons H24 and H25 of the ethyl group pointing on the oxygen side are far from the pyridyl ring and do not exhibit any NOE with the H3 proton. A weak NOE is also observed between one proton of a lateral pyridine ring (H16) and one ethyl proton (H31) of the ring, showing that the oxygen atom and the nitrogen atom of the pyridyl group can be oriented on the same side. Two possibilities can be suggested to explain these NOEs. First, a cis−trans conformation could be exclusively present in solution (Figure 4) and would explain all of the NOEs observed. Second, the NOEs could reflect the flexibility of the molecule and the possible rotations of the pyridine rings or the amide groups along the C−C bonds. In that case, a mixture of all the ring conformations (cis−cis, cis−trans, or trans−trans) can exist in solution.

In the presence of HCl, most of the NOEs vanish except between the protons of the two adjacent pyridine rings (H5 and H18 or H3 and H12). The conformation of the protonated te-tpyda is thus mainly cis−cis with respect to the pyridine rings.

*DFT Calculations on Free Forms of tpy and te-tpyda.* DFT calculations were performed on the free molecules in their protonated and unprotonated forms in order to determine their preferred conformation. The energy differences between the


dx.doi.org/10.1021/ic200271e |*Inorg. Chem.* 2011, 50, 6557–6566

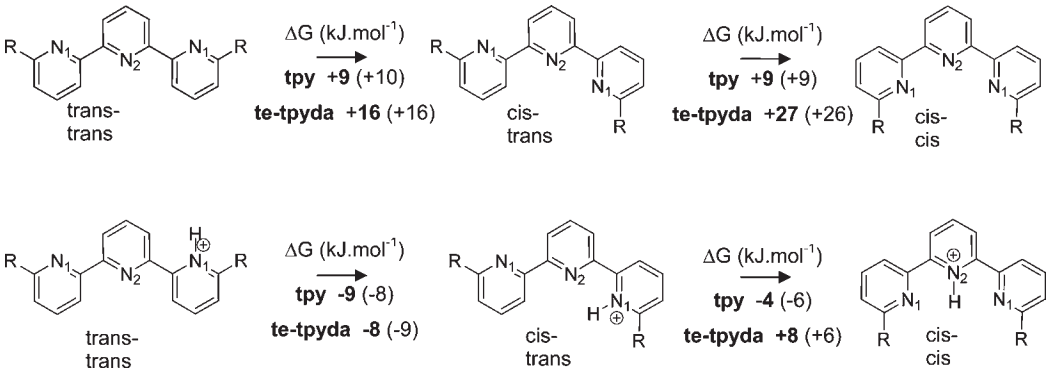


**Figure 5.** Conformations of the unprotonated (top) and monoprotonated (bottom) forms of tpy and te-tpyda. Free energy differences $\Delta G$ in kJ·mol$^{-1}$ obtained from DFT (B3LYP) calculations with a continuum solvent model corresponding to $H_2O$ and MeOH (values in parentheses).

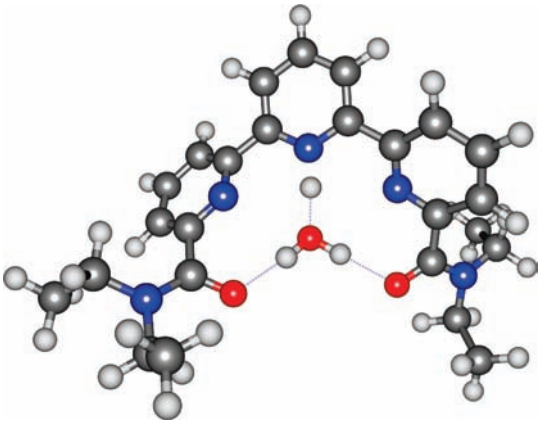

**Figure 6.** Conformation of the monoprotonated form of te-tpyda with one $H_2O$ molecule obtained from DFT (B3LYP) calculations.

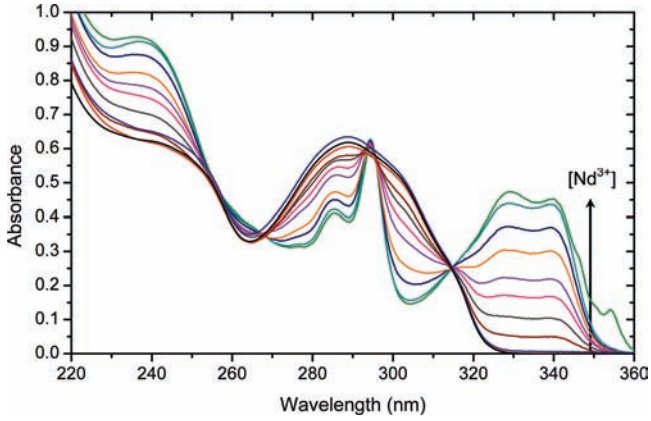


**Figure 7.** Spectrophotometric titration of a 2.5 × 10$^{-5}$ mol·L$^{-1}$ te-tpyda solution with increasing concentrations of $Nd^{3+}$ in 75/25 vol % MeOH/$H_2O$ at 21 °C. Path length: 1 cm. 0 < [$Nd^{3+}$]/[te-tpyda] < 1330.

three conformations of the pyridine rings of tpy and te-tpyda (unprotonated and monoprotonated forms) were computed. The solvent ($H_2O$ or MeOH) was modeled through a continuum dielectric medium. The results are shown in Figure 5. As reported for tpy,[28−31] the preferred conformations for the unprotonated tpy and te-tpyda are trans−trans in $H_2O$ and MeOH. For te-tpyda, this is in disagreement with the NMR results, which indicate the presence either of the cis−trans conformation only or of a mixture of conformations. However, as shown for tpy,[29] solvent molecules may further stabilize the cis−cis conformation by creating intermolecular hydrogen bonds between one solvent molecule and the two lateral nitrogen atoms. These specific interactions are not properly described by the continuous solvent model with no explicit $H_2O$ or MeOH solvent molecules. For the monoprotonated tpy molecules, the most stable structure is the cis−cis conformation with a hydrogen atom at the central pyridine ring. However, this structure is very close in energy to the cis−trans conformation, with a hydrogen atom located on a lateral pyridine ring. Considering the small energy gap between the two conformations (4−6 kJ·mol$^{-1}$), both forms may exist in solution or a specific interaction in a medium should be taken into account to stabilize one form over the other. This is consistent with the NMR experiments, which have pointed out the possible existence of both conformations for monoprotonated tpy.[30,31] For te-tpyda, the lowest-energy structure is the cis−trans one, but energy differences between the three conformations are also small. In order to have the cis−cis conformation as the most stable form, as observed by NMR, it is necessary to add an explicit $H_2O$ molecule in the calculation (optimized structure shown in Figure 6). The cis−cis structure is then strongly stabilized by the presence of two hydrogen bonds between the hydrogen and oxygen atoms from the two C═O. This specific hydrogen-bond interaction is induced by the carbonyl groups and does not exist for tpy. Overall, these results show that solvation plays a key role with the formation of specific hydrogen-bond interactions, which may stabilize one form over another.

**Complexation of Lanthanides and Actinides by Terpyridinediamides.** *Stability Constants.* The stability constants ($\beta_1$) for complexation by te-tpyda, dedp-tpyda, and tpy of some lanthanide cations ($La^{3+}$, $Nd^{3+}$, $Eu^{3+}$, and $Yb^{3+}$) were determined by UV−visible spectrophotometry in a 75/25 vol % MeOH/$H_2O$ solution by following the absorption of the ligand. A sample spectrophotometric titration of te-tpyda by $Nd^{3+}$ is shown in Figure 7, whereas other experimental spectra are available in the Supporting Information. Stability constants $\beta_1$ were calculated from each set of UV absorption spectra over a wavelength range of 200−400 nm using *Hyperquad 2006* for equilibrium (2), which is appropriate because the spectrophotometric data support the formation of only the 1:1 $Ln^{III}$/ligand


dx.doi.org/10.1021/ic200271e |*Inorg. Chem.* 2011, 50, 6557–6566

complex for all of the cations and the ligand studied.

$$Ln^{3+} + \text{te-tpyda} \overset{\beta_1}{\rightleftharpoons} Ln(\text{te-tpyda})^{3+} \quad (2)$$

The stability constants ($\beta_1$) for the $UO_2$(te-tpyda) and Am(te-tpyda) complexes were determined by following the absorption of the actinide cation and by adding increasing concentrations of te-tpyda in solution. A sample spectrophotometric titration of $Am^{3+}$ by te-tpyda is depicted in Figure 8, while UV−visible spectra corresponding to $UO_2^{2+}$ titration are reported in the Supporting Information.

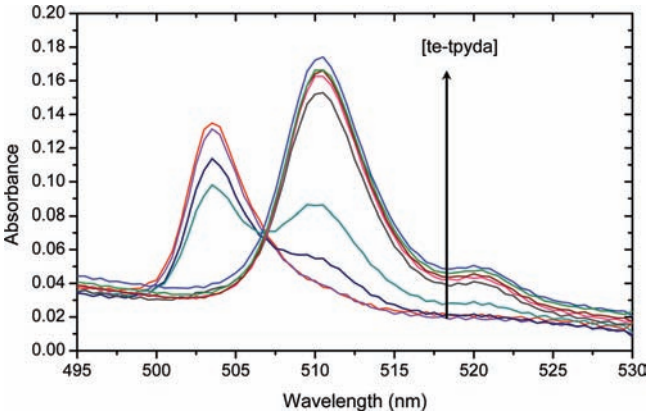


**Figure 8.** Spectrophotometric titration of a $3.3 \times 10^{-4}$ mol·L$^{-1}$ $Am^{3+}$ solution with increasing concentrations of te-tpyda in 75/25 vol % MeOH/$H_2O$ at 21 °C. Path length: 1 cm. $0 < [\text{te-tpyda}]/[Am^{3+}] < 100$.

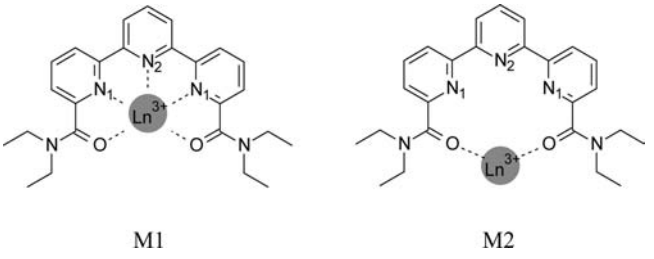


**Figure 9.** Structures of coordination modes M1 and M2 for the $Ln^{III}$/(te-tpyda) complex.

All measured stability constants are reported in Table 2. The log $\beta_1$ values corresponding to the complexation of lanthanides by te-tpyda vary between 2.7 and 4.5 and are significantly higher (1 to 2 orders of magnitude) than those of nonfunctionalized tpy. The 1:1 complex formed with dedp-tpyda and europium is more stable than the corresponding complex with te-tpyda ($\log \beta_{1Eu(\text{dedp-tpyda})} - \log \beta_{1Eu(\text{te-tpyda})} = 0.5$). The stability constant of the Nd(te-tpyda) complex was also determined by a spectrophotometric titration of Nd by te-tpyda. The absorption of $Nd^{III}$ was followed between 400 and 900 nm, by keeping constant the $Nd^{3+}$ concentration and adding increasing concentrations of the ligand. The log $\beta_1$ values estimated by each of these two sets of spectrophotometric experiments (Table 2) show a slight difference, but the order of magnitude is consistent whatever the titration mode is. The log $\beta_1$ value for the $Am^{3+}$ complex is significantly higher than the corresponding constant with $UO_2^{2+}$ ($\log \beta_{1Am(\text{te-tpyda})} - \log \beta_{1UO_2(\text{te-tpyda})} = 1.6$) but is very close to the $Nd^{3+}$ constant determined in the same conditions.

*MD Simulations.* The te-tpyda ligand may adopt two possible coordination modes toward the cations. The ligand could be first pentadentate (coordination M1) with the three pyridine nitrogen atoms and two oxygen atoms being directly coordinated to the cation. In the second possible coordination mode (M2), only the two oxygen atoms would be in the first coordination sphere of the cation. Conformations M1 and M2 of $Nd^{3+}$ and $Dy^{3+}$ complexes formed with te-tpyda in $H_2O$ or in MeOH were studied using MD simulations. For both lanthanide cations, almost the same structural properties were determined in pure $H_2O$ and neat MeOH. By calculation, it appears that the lanthanide cation is outside the nitrogen cavity in both $H_2O$ and MeOH, i.e., going from the M1 conformation to the M2 conformation represented in Figure 9.

In $H_2O$, the terpyridinediamide molecule would be coordinated to $Ln^{3+}$ only through the two carbonyl oxygen atoms (Figure 10, left), with average $Ln^{3+}-O_{CO}$ distances equal to 2.50 and 2.37 Å for $Nd^{3+}$ and $Dy^{3+}$, respectively. The lanthanide first coordination shell is filled by $H_2O$ molecules: seven for $Nd^{3+}$ ($d_{Nd-Ow}^{(1)} = 2.53$ Å) and six for $Dy^{3+}$ ($d_{Dy-Ow}^{(1)} = 2.39$ Å). Some of the $Ln^{3+}$ first coordination shell $H_2O$ molecules make hydrogen bonds with the terpyridine nitrogen atoms, stabilizing the M2 conformation. As expected from previous studies on

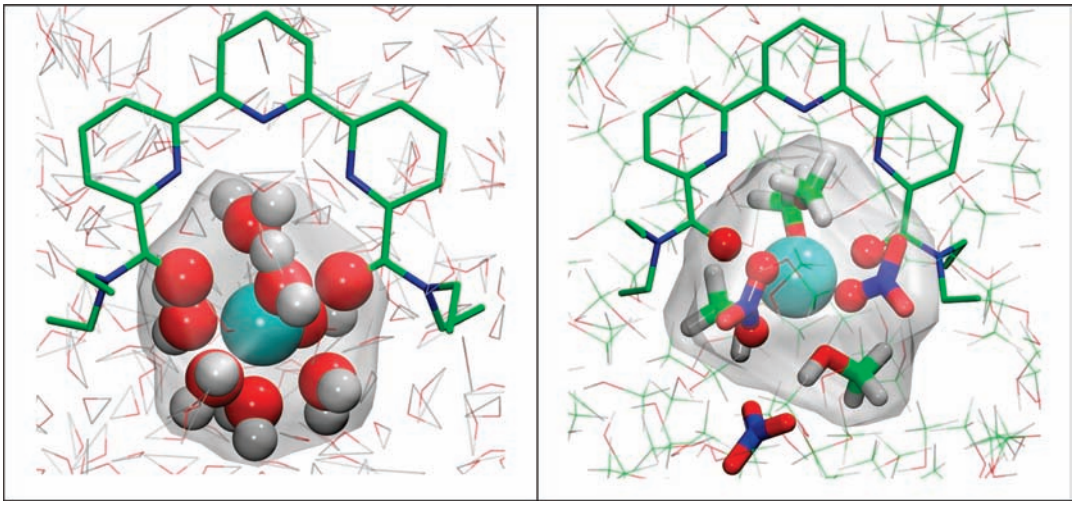

**Figure 10.** MD simulation snapshots of $Nd^{3+}$ complexes in pure $H_2O$ (left) and neat MeOH (right).


dx.doi.org/10.1021/ic200271e |*Inorg. Chem.* 2011, 50, 6557–6566

lanthanide nitrate salts,[20] the nitrate ions are fully dissociated. In MeOH, the lanthanide cations are also located outside the nitrogen cavity (Figure 10, right), in the M2 conformation. However, contrary to pure $H_2O$ simulations, nitrate anions are observed in the $Ln^{3+}$ first coordination shell with both monodentate and bidentate coordination modes.

*DFT Calculations.* The binding properties of te-tpyda toward neodymium and americium were investigated through DFT calculations. Nd and Am were selected because of their similar size. The geometries of neodymium and americium complexes with one ligand and $H_2O$ molecules in their coordination sphere were optimized for the two coordination modes M1 and M2. The metal ions were considered as being nine-coordinate in solution, and $H_2O$ molecules were added around the metal in order to complete its first coordination sphere. Because the ligand is pentadentate in M1 and bidentate in M2, four and seven $H_2O$ molecules were added in M1 and M2, respectively. Furthermore, in order to compare the energies between the two coordination modes, it is necessary to have the same stoichiometry in the two M1 and M2 structures. Therefore, for the M1 coordination mode, three $H_2O$ molecules were also added in the second coordination sphere in order to have a total number of seven $H_2O$ molecules for M1 and M2. Energy differences between the two coordination modes are reported in Table 3. Energies in solution were obtained using a polarizable continuum model. For all of the cations and at all levels of calculations, the M1 coordination mode is systematically lower in energy than M2 by 80−110 kJ·mol$^{-1}$ in the gas phase and by 30−60 kJ·mol$^{-1}$ in solution. $Nd^{3+}$ and $Am^{3+}$ have similar ionic radii, but the energy difference between M1 and M2 is larger for americium than for neodymium by about 20 kJ·mol$^{-1}$ (SC calculations). This indicates a higher binding affinity of the nitrogen cavity for americium than for neodymium. The free-energy change of reaction (3) was calculated for M1 and M2.

$$\mathrm{Nd(te\text{-}tpyda)(H_2O)_9}^{3+} + \mathrm{Am(H_2O)_9}^{3+} \rightarrow \mathrm{Am(te\text{-}tpyda)(H_2O)_9}^{3+} + \mathrm{Nd(H_2O)_9}^{3+} \quad (3)$$

This reaction was chosen to encourage error cancellation. Its energy variation is very helpful in quantifying the relative affinity of the ligand for neodymium versus americium. Because $Nd^{3+}$ and $Am^{3+}$ have similar ionic radii, solvation and entropy effects should be similar for each side of the reaction. When te-tpyda binds $Nd^{3+}$ and $Am^{3+}$ through the nitrogen atoms of the pyridine rings (M1), the free-energy change of reaction (2) is negative by −12 kJ·mol$^{-1}$ (Table 3). This indicates that the nitrogen cavity of te-tpyda should bind $Am^{3+}$ more strongly than $Nd^{3+}$. On the other hand, when the nitrogen cavity is not directly involved in the chelation (M2), the reaction energy becomes slightly positive. As expected, the calculated energy of the reaction is similar in the gas phase and in solution because both cations undergo comparable bulk solvation effects. The preference of the nitrogen cavity for amercium over neodymium disappears when the 5f-in-core and 4f-in-core pseudopotentials are used. This may indicate that 5f orbitals play a role in the binding of $Am^{3+}$ inside the nitrogen cavity. A natural population analysis of the wave function calculated with small-core pseudopotentials reveals a small increase of the 5f and 6d populations from neodymium to americium, as was observed on similar systems.[32−34] Yet, very small energy differences are found between neodymium and americium, and it is very difficult to determine accurately the ligand binding energy toward an open-shell actinide because of the near-degeneracy of f orbitals and the resulting manifold of low-lying excited states involving $5f^n$ configurations. A multiple-reference wave function, including all possible f occupations, is more appropriate than a single-reference DFT approach to treat the near-degenerence of 5f orbitals. Accurate multiple-reference calculations were reported on trivalent cerium and uranium with N-heterocyclic carbenes and showed that DFT (with 5f-in-valence pseudopotential) predicts the correct sign for relative binding energies but overestimates by more than 10 kJ·mol$^{-1}$ the preference for uranium over cerium.[35] This means that if the cations are inside the nitrogen cavity (M1), the energy difference for an americium/neodymium exchange reaction could be even smaller than −12 kJ·mol$^{-1}$.

**Table 3. Free-Energy Differences $\Delta G$ between M1 and M2 Structures and for the Nd → Am Exchange Reaction[a]**

| | method | gas | solution |
|---|---|---|---|
| Nd[b] | LC | +81 | +26 (31) |
| Nd[b] | SC | +87 | +34 (39) |
| Am[b] | LC | +84 | +30 (38) |
| Am[b] | SC | +109 | +57 (65) |
| Nd → Am M1[c] | SC | −13 | −12 |
| Nd → Am M1[c] | LC | +5 | +5 |
| Nd → Am M2[c] | SC | +10 | +11 |
| Nd → Am M2[c] | LC | +8 | +9 |

[a] Values in kJ·mol$^{-1}$ calculated at the B3LYP level in the gas phase and in solution using a continuum solvent model for $H_2O$ (values in MeOH in parentheses). LC and SC correspond to large-core (4f or 5f in core) and small-core (4f or 5f in valence) pseudopotentials, respectively. [b] $ML(H_2O)_4(H_2O)_3^{3+}$ (M1) → $ML(H_2O)_7^{3+}$ (M2). [c] $Nd(L)(H_2O)_9^{3+} + Am(H_2O)_9^{3+} \rightarrow Am(L)(H_2O)_9^{3+} + Nd(H_2O)_9^{3+}$.

*UV−Visible Spectra (TD-DFT Calculations).* The UV−visible spectra corresponding to ligand transitions were simulated using the TD-DFT approach for the free ligand and neodymium complexes in both coordination modes. TD-DFT has become a standard tool for computing vertical transitions in the UV−visible region for organic molecules and metal complexes. $\lambda_{max}$ corresponding to $\pi-\pi^*$ transitions in an organic molecule can be well reproduced through this calculation approach, which was successfully applied to lanthanide−terpyridine complexes.[36]

Experimental and theoretical studies of UV absorption spectra were reported for tpy systems.[28,30,31,36] The UV spectra of free ligands in their unprotonated form are dominated by a first large absorption band at around 280−290 nm corresponding to $\pi-\pi^*$ transitions and a second band at smaller wavelength at around 230 nm. Protonation or metal chelation of tpy is accompanied with the appearance of a red-shifted absorption band. Therefore, in an acidic solution or in the presence of a metal cation, the spectra exhibit three bands around 340−320, 285−270, and 240−220 nm.[30] For the two longer-wavelength bands, satellite bands are observed and were attributed to vibrational fine structures.

TD-DFT-calculated transition energies with high oscillator strengths are given in Table 3. They were determined for te-tpyda in its free unprotonated form (in trans−trans and cis−cis conformations) and in neodymium complexes. All of the transition energies correspond to $\pi-\pi^*$ transitions localized on the te-tpyda ligand. The experimental spectrum of te-tpyda in the absence of neodymium shows a large absorption band with a


dx.doi.org/10.1021/ic200271e |*Inorg. Chem.* 2011, 50, 6557–6566

Table 4. Absorption Wavelength (in nm) and Oscillator Strengths *f* Obtained from TD-DFT (B3LYP) Calculations in $H_2O$ for te-tpyda (in Trans−Trans, Cis−Trans, and Cis−Cis Conformations) and for Nd(te-tpyda)$(H_2O)_n^{3+}$ Complexes in M1 ($n = 4$) and M2 ($n = 7$)[a]

| te-tpyda (trans−trans) | | te-tpyda (cis−trans) | | te-tpyda (cis−cis) | | Nd(te-tpyda) (M1) | | Nd(te-tpyda) (M2) | |
|---|---|---|---|---|---|---|---|---|---|
| $\lambda$ | $f$ | $\lambda$ | $f$ | $\lambda$ | $f$ | $\lambda$ | $f$ | $\lambda$ | $f$ |
| 305 | 0.28 | 299 | 0.10 | 289 | 0.19 | 322 | 0.34 | 309 | 0.28 |
| 291 | 0.07 | 297 | 0.09 | 277 | 0.09 | 296 | 0.19 | 288 | 0.20 |
| 289 | 0.16 | 292 | 0.15 | 276 | 0.05 | 279 | 0.06 | 277 | 0.12 |
| 282 | 0.19 | 277 | 0.07 | 271 | 0.12 | 273 | 0.13 | 272 | 0.07 |
| 276 | 0.06 | 275 | 0.07 | 271 | 0.07 | | | | |

[a] Only transitions with *f* larger than 0.05 and with $\lambda$ longer than 270 nm are reported.

maximum at ∼290 nm and a shoulder at ∼305 nm (Figure 7). The shoulder at 305 nm can be attributed to the trans−trans conformation whose absorption maximum is calculated at 305 nm with some participation of the cis−trans conformation (Table 4). The maximum at ∼290 nm can be attributed to any of the conformations. According to the calculations, a change from the trans−trans to cis−cis conformation is associated with a blue shift from 10 to 15 nm for the most intense transitions. The broad shape of the experimental spectrum is most likely related to the flexibility of the three pyridine rings and suggests the presence of the three conformations in solution. According to the calculations, the spectral signature of te-tpyda when bound to neodymium in M2 is very similar to the one for free te-tpyda. In the experimental spectrum, neodymium complexation with te-tpyda is associated with the appearance of a red-shifted absorption band. According to the calculations, it is only when te-tpyda is bound to neodymium through its nitrogen atoms (M1) that a high-intensity transition appears at longer wavelength (>320 nm). As described for tpy,[37] the splitting of the lowest-energy absorption band into two features can be attributed to vibronic effects, which are not taken into account in these calculations.

## DISCUSSION

**Ligand Protonation.** The protonation constants of the new bitopic ligands te-tpyda and dedp-tpyda were measured and compared to those of the nonfunctionalized tpy. The lower value of the first p*K* of the functionalized tpy ($pK_1 = 1.0$; 2 orders of magnitude lower than the $pK_1$ of tpy) coupled with the observation of only one protonation clearly shows that adding alkylamide functional groups on the tpy moiety significantly lowers the basicity of the pyridyl nitrogen atoms. This result explains the good performances observed with these ligands in solvent extraction experiments at high acidity.[11] However, the substitution of an ethyl group by a phenyl has no influence on the molecule basicity because the log $K_{1H}$ values for te-tpyda and dedp-tpyda are equal within uncertainty. According to $^{15}N-^{1}H$ NMR correlation spectra, the protonation of the pyridyl nitrogen atoms differs from tpy to te-tpyda. Indeed, the protonation disturbs mainly the central nitrogen atom and the lateral nitrogen atoms are not involved, while the reverse phenomenon is observed with the tpy protonation. This experimental evidence emphasizes the decreasing basicity that occurs when tpy is functionalized with amide groups. The multiple NOEs observed by NMR show that the unprotonated te-tpyda ligand may adopt different conformations in a $MeOH/H_2O$ solution. This highlights the relative flexibility of the molecule and the possible rotation of the pyridine rings along the C−C bonds, while the trans−trans conformation of the unprotonated tpy ligand should be predominant.[28−31] According to $^{1}H$ NMR, the protonation of te-tpyda leads to the cis−cis conformation in which pyridine rings draw a cavity made of three nitrogen atoms. DFT calculations suggest that this cis−cis protonated form with hydrogen at the central nitrogen atom can be stabilized by the presence of $H_3O^+$ inside the cavity, which creates two hydrogen bonds with the oxygen atoms of the amide functional groups. In the case of tpy, previous theoretical[29,31] and experimental studies (UV−visible spectrophotometry in aqueous solution,[30] NMR in acetonitrile,[31] and crystal structures[31,38]) have shown that the monoprotonated ligand could adopt both the cis−cis and cis−trans forms depending on the medium and the presence or absence of solvents and/or anions, which can accept hydrogen bonding. In the present work, the calculations show that, for te-tpyda molecules, solvation plays a key role with the formation of specific hydrogen-bond interactions, which may stabilize the cis−cis form over others.

**Lanthanide Complexation.** The stability constants for the 1:1 Ln(te-tpyda) complexes seem to vary non-monotonically across the lanthanide series: the stability increases from lanthanum to europium and then decreases in the end of the series. Therefore, the trends across the series cannot be explained only by an ionic interaction but by a compromise between the decrease of the ionic radius, the coordination number through the lanthanide series, and the size of the coordination cavity of the ligand. The comparison of the stability constants of te-tpyda lanthanide complexes with nonfunctionalized tpy reported in Table 2 shows that te-tpyda complexes are much more stable than tpy complexes under the same conditions. These results emphasize the impact of the addition of the alkylamide groups on the complexing properties of the ligand. All other things being equal, the drop in basicity of the tridentate tpy should induce a decrease in the affinity of the ligand toward cations. However, this effect is offset by the addition of two oxygen donors. The ligand is then pentadentate and has a higher affinity for lanthanide cations than tpy. The combination of both effects is very interesting with respect to new ligands for solvent extraction of actinide cations from concentrated acidic solutions. More acidic ligands can lead to stronger extractants because this minimizes the proton−metal competition in these systems. This work shows that these new bitopic N,O systems present a way to decrease the basicity of the ligand, while increasing its intrinsic metal affinity, hence improving the extractability of metals from acidic solutions.[11] The higher $\beta_1$ constant measured for the Eu(dedp-tpyda) complex compared


dx.doi.org/10.1021/ic200271e |*Inorg. Chem.* 2011, 50, 6557–6566

to Eu(te-tpyda) shows that substitution of an ethyl group by a phenyl enhances the stability of the europium complex. The increase in stability could be attributed to the electronic (driven by enthalpy) or steric (driven by entropy) properties. This effect has already been observed in the literature with other ligands and is called the "anomalous aryl strengthening".[39−42]

In the case of $Nd^{III}$, the stability constant of Nd(te-tpyda) was determined by following both the absorbance of the ligand in UV and the absorbance of $Nd^{3+}$ in the visible region. The relatively good agreement between both sets of experiments confirms the 1:1 stoichiometry. The measured spectral modifications accompanying neodymium complexation upon ligand addition have been observed for complexes of tpy and are characteristic of inner-sphere complexation.[37] These variations were attributed to rigidification of the ligand upon complex formation.

Besides, distinct spectral modifications of the Nd 4f−4f absorption band upon complexation are evidence of inner-sphere coordination. DFT calculations and MD simulations were performed upon Nd(te-tpyda) complexation and show that two coordination modes corresponding to an inner-sphere coordination can exist in solution. In one structure (M1), te-tpyda is pentadentate and binds the cation through the three nitrogen and two oxygen atoms. In the second structure (M2), only carbonyl groups are directly bound to lanthanide cations and nitrogen atoms are only bound through hydrogen-bound $H_2O$ molecules. Static DFT calculations disfavor the M2 coordination mode, but MD simulations with explicit solvent molecules show that the dynamic of $H_2O$ molecules may have a strong effect on the preferred coordination mode and favors the M2 mode rather than M1. Determination of the preferred coordination mode from these calculations is, however, very difficult. Indeed, in MD simulations, which take into account explicitly the solvent and its effects on the structures, the potential includes the polarization effects, but not the charge-transfer ones, that may favor the M1 coordination mode. In static DFT calculations, the cation interactions with the ligands are not precisely calculated, but the solvent effects, which favor M2 coordination, are less taken into account.

In order to determine which structure is predominant in solution, the UV−visible spectrum was measured and simulated from TD-DFT for the Nd(te-tpyda) complex for both coordination modes because both modes cause rigidification of the ligand upon complex formation and could induce the observed UV spectral evolutions. In the experimental spectrum, neodymium complexation with te-tpyda is associated with the appearance of a red-shifted absorption band. According to the calculations, it is only when te-tpyda binds neodymium through its nitrogen atoms (M1) that a high-intensity transition appears at a longer wavelength. Therefore, the spectral evolutions strongly suggest a M1 coordination mode in $MeOH/H_2O$ conditions.

**Actinide Complexation.** Although more stable complexes were expected with actinide cations, equal or lower stability constants were measured for $U^{VI}$ and Am(te-tpyda) complexes compared to $Ln^{III}$ complexes. The selectivity observed in solvent-extraction experiments (in an octanol diluent)[11] was therefore not confirmed by these experiments in a homogeneous $MeOH/H_2O$ medium. The relatively low $\log \beta_1$ value for the U(te-tpyda) complex ($\log \beta_1 = 2.2$) could arise from an incomplete coordination of the donor atoms.

A comparison between the americium and neodymium complexes (with cations having similar size and hydration properties) shows a very close stability and does not highlight any selectivity for americium. The americium/neodymium selectivity observed with adptz, a pure nitrogen-donor ligand, in the same experimental conditions,[27] does not occur in the case of te-tpyda, a N,O-bearing ligand. According to DFT calculations, only a binding in the nitrogen cavity can induce selectivity and te-tpyda should bind more strongly americium than neodymium but by a very small amount of energy, a few kilojoules per mole, which cannot be quantified precisely. Because analysis of UV spectra ruled out the presence of the M2 conformations in solution, the lack of americium/neodymium selectivity would appear to be due to a lack of selectivity in the nitrogen cavity.

As observed previously with lanthanides, the addition of ethylamide groups on the tpy moiety enhances the stability of the americium complex by a factor of 2.5 ($\log \beta_{1(AmTpy)} = 3.4$).[27] The impact is, however, smaller than that with the lanthanide cations.

## CONCLUSION

The complexation of uranium(VI), americium(III), and lanthanides(III) (La, Nd, Eu, and Yb) with new bitopic N,O ligands was studied in homogeneous $MeOH/H_2O$ conditions. The protonation and stability constants of terpyridinediamide ligands with $U^{VI}$, $Am^{III}$, and $Ln^{III}$ were measured using UV−visible spectrophotometry and compared with nonfunctionalized tpy. The addition of amide groups on the tpy moiety lowers the basicity of the ligand and enhances the stability of the complexes, thus confirming the faculty of these ligands to extract actinides from highly acidic media. However, the $An^{III}/Ln^{III}$ selectivity shown in solvent extraction with long-chain terpyridinediamides was not confirmed in solution when the $Am^{III}$ and $Nd^{III}$ stability constants were compared in the case of te-tpyda.

NMR experiments show that the unique protonation of the ligand occurs on the central nitrogen atom of the tpy moiety, and DFT calculations predict that the corresponding cis−cis structure is stabilized by solvation effects. Coordination of the ligands was studied by DFT and MD calculations.

Two possible inner-sphere coordination modes were found from the calculations: one mode where the cation is coordinated by the nitrogen atoms of the cavity and by the amide oxygen atoms and one mode where the cation is only coordinated by the two amide oxygen atoms and by solvent molecules. The lack of americium/neodymium selectivity could be due either to a lack of selectivity of the nitrogen cavity and/or to the presence of M2 conformations in the solution. However, the second possibility was ruled out from analysis of the UV−visible spectra.

## ASSOCIATED CONTENT

**Supporting Information.** UV−visible experimental, NMR spectra, and MD data. This material is available free of charge via the Internet at http://pubs.acs.org.

## AUTHOR INFORMATION

### Corresponding Author

*E-mail: manuel.miguirditchian@cea.fr. Tel.: +33466339009. Fax: +33438785090.

## REFERENCES

(1) Pearson, R. G. *J. Am. Chem. Soc.* **1963**, *85* (22), 3533–3539.
(2) Rizkalla, E. N.; Choppin, G. R. *J. Alloys Compd.* **1992**, *180* (1−2), 325–336.

(3) David, F. *J. Less-Common Met.* **1986**, *121*, 27–42.
(4) Shannon, R. *Acta Crystallogr., Sect. C* **1976**, *32* (5), 751–767.
(5) Hill, C.; Madic, C.; Baron, P.; Ozawa, M.; Tanaka, Y. *J. Alloys Compd.* **1998**, *271*−*273*, 159–162.
(6) Ionova, G.; Ionov, S.; Rabbe, C.; Hill, C.; Madic, C.; Guillaumont, R.; Krupa, J. C. *Solvent Extr. Ion Exch.* **2001**, *19* (3), 391–414.
(7) Miyashita, S.; Yanaga, M.; Satoh, I.; Suganuma, H. *Chem. Lett.* **2006**, *35* (2), 236–237.
(8) Miyashita, S.; Yanaga, M.; Satoh, I.; Suganuma, H. *J. Nucl. Sci. Technol.* **2007**, *44* (2), 233–237.
(9) Kolarik, Z. *Chem. Rev.* **2008**, *108* (10), 4208–4252.
(10) Nash, K. L. *Solvent Extr. Ion Exch.* **1993**, *11* (4), 729–768.
(11) Marie, C.; Miguirditchian, M.; Guillaneux, D.; Bisson, J.; Pipelier, M.; Dubreuil, D. *Solvent Extr. Ion Exch.* **2011**, *29* (2), 292–315.
(12) Frassineti, C.; Ghelli, S.; Gans, P.; Sabatini, A.; Moruzzi, M.; Vacca, A. *Anal. Biochem.* **1995**, *231*, 374–382.
(13) Frisch, M. J.; Trucks, G. W.; Schlegel, H. B.; Scuseria, G. E.; Robb, M. A.; Cheeseman, J. R.; Montgomery, J. A., Jr.; Vreven, T.; Kudin, K. N.; Burant, J. C.; Millam, J. M.; Iyengar, S. S.; Tomasi, J.; Barone, V.; Mennucci, B.; Cossi, M.; Scalmani, G.; Rega, N.; Petersson, G. A.; Nakatsuji, H.; Hada, M.; Ehara, M.; Toyota, K.; Fukuda, R.; Hasegawa, J.; Ishida, M.; Nakajima, T.; Honda, Y.; Kitao, O.; Nakai, H.; Klene, M.; Li, X.; Knox, J. E.; Hratchian, H. P.; Cross, J. B.; Bakken, V.; Adamo, C.; Jaramillo, J.; Gomperts, R.; Stratmann, R. E.; Yazyev, O.; Austin, A. J.; Cammi, R.; Pomelli, C.; Ochterski, J. W.; Ayala, P. Y.; Morokuma, K.; Voth, G. A.; Salvador, P.; Dannenberg, J. J.; Zakrzewski, V. G.; Dapprich, S.; Daniels, A. D.; Strain, M. C.; Farkas, O.; Malick, D. K.; Rabuck, A. D.; Raghavachari, K.; Foresman, J. B.; Ortiz, J. V.; Cui, Q.; Baboul, A. G.; Clifford, S.; Cioslowski, J.; Stefanov, B. B.; Liu, G.; Liashenko, A.; Piskorz, P.; Komaromi, I.; Martin, R. L.; Fox, D. J.; Keith, T.; Al-Laham, M. A.; Peng, C. Y.; Nanayakkara, A.; Challacombe, M.; Gill, P. M. W.; Johnson, B.; Chen, W.; Wong, M. W.; Gonzalez, C.; Pople, J. A. *Gaussian 03*, revision D.02; Gaussian, Inc.: Wallingford, CT, 2004.
(14) Cao, X.; Dolg, M. *THEOCHEM* **2002**, *581* (1−3), 139–147.
(15) Cao, X.; Dolg, M.; Stoll, H. *J. Chem. Phys.* **2003**, *118* (2), 487–496.
(16) Dolg, M.; Stoll, H.; Savin, A.; Preuss, H. *Theor. Chim. Acta* **1989**, *75*, 173–194.
(17) Wiebke, J.; Moritz, A.; Cao, X.; Dolg, M. *Phys. Chem. Chem. Phys.* **2007**, *9* (4), 459–465.
(18) Case, D. A. AMBER 8.
(19) Darden, T.; York, D.; Pedersen, L. *J. Chem. Phys.* **1993**, *98* (12), 10089–10092.
(20) Duvail, M.; Ruas, A.; Venault, L.; Moisy, P.; Guilbaud, P. *Inorg. Chem.* **2010**, *49* (2), 519–530.
(21) Clavaguéra, C.; Dognon, J.-P. *J. Chem. Phys.* **2005**, *311*, 169–176.
(22) Caldwell, J. W.; Kollman, P. A. *J. Phys. Chem.* **1995**, *99*, 6208–6219.
(23) Meng, E. C.; Kollman, P. A. *J. Phys. Chem.* **1996**, *100* (27), 11460–11470.
(24) Jorgensen, W. L.; Maxwell, D. S.; Tirado-Rives, J. *J. Am. Chem. Soc.* **1996**, *118* (45), 11225–11236.
(25) Yu, H.; Geerke, D. P.; Liu, H.; van Gunsteren, W. E. *J. Comput. Chem.* **2006**, *27*, 1494–1504.
(26) Bayly, C. I.; Cieplak, P.; Cornell, W.; Kollman, P. A. *J. Phys. Chem.* **1993**, *97* (40), 10269–10280.
(27) Miguirditchian, M.; Guillaneux, D.; François, N.; Airvault, S.; Ducros, S.; Thauvin, D. *Nucl. Sci. Eng.* **2006**, *153*, 223–232.
(28) Bazzicalupi, C.; Bencini, A.; Bianchi, A.; Danesi, A.; Faggi, E.; Giorgi, C.; Santarelli, S.; Valtancoli, B. *Coord. Chem. Rev.* **2008**, *252* (10−11), 1052–1068.
(29) Drew, M. G. B.; Hudson, M. J.; Iveson, P. B.; Russell, M. L.; Liljenzin, J.-O.; Skalberg, M.; Spjuth, L.; Madic, C. *J. Chem. Soc., Dalton Trans.* **1998**, *18*, 2973–2980.
(30) Nakamoto, K. *J. Chem. Phys.* **2002**, *64* (10), 1420–1425.
(31) Yoshikawa, N.; Yamabe, S.; Kanehisa, N.; Inoue, T.; Takashima, H.; Tsukahara, K. *J. Phys. Org. Chem.* **2010**, *23* (5), 431–439.
(32) Miguirditchian, M.; Guillaneux, D.; Guillaumont, D.; Moisy, P.; Madic, C.; Jensen, M. P.; Nash, K. L. *Inorg. Chem.* **2005**, *44* (5), 1404–1412.
(33) Ingram, K. I. M.; Tassell, M. J.; Gaunt, A. J.; Kaltsoyannis, N. *Inorg. Chem.* **2008**, *47* (17), 7824–7833.
(34) Guillaumont, D. *J. Phys. Chem. A* **2004**, *108* (33), 6893–6900.
(35) Gagliardi, L.; Cramer, C. J. *Inorg. Chem.* **2006**, *45* (23), 9442–9447.
(36) Gutierrez, F.; Rabbe, C.; Poteau, R.; Daudey, J. P. *J. Phys. Chem. A* **2005**, *109* (19), 4325–4330.
(37) Hamilton, J. M.; Anhorn, M. J.; Oscarson, K. A.; Reibenspies, J. H.; Hancock, R. D. *Inorg. Chem.* **2011**, *50* (7), 2764–2770.
(38) Hergold-Brundic, A.; Popovic, Z.; Matkovic-Calogovic, D. *Acta Crystallogr., Sect. C* **1996**, *52* (12), 3154–3157.
(39) Paulenova, A.; Alyapyshev, M. Y.; Babain, V. A.; Herbst, R. S.; Law, J. D. *Sep. Sci. Technol.* **2008**, *43* (9), 2606–2618.
(40) Babain, V. A.; Alyapyshev, M. Y.; Kiseleva, R. N. *Radiochim. Acta* **2007**, *95* (4), 217–223.
(41) Babain, V.; Alyapyshev, M.; Smirnov, I.; Shadrin, A. *Radiochemistry* **2006**, *48* (4), 369–373.
(42) Alyapyshev, M. Y.; Babain, V. A.; Borisova, N. E.; Kiseleva, R. N.; Safronov, D. V.; Reshetova, M. D. *Mendeleev Commun.* **2008**, *18* (6), 336–337.